Journal of Cystic Fibrosis xxx (xxxx) xxx

Contents lists available at ScienceDirect

Journal of Cystic Fibrosis

journal homepage: www.elsevier.com/locate/jcf

Original Article

A W1282X cystic fibrosis mouse allows the study of pharmacological and gene-editing therapeutics to restore CFTR function

Margaret Michicich, Zachary Traylor, Caitlan McCoy, Dana M. Valerio, Alma Wilson, Molly Schneider, Sakeena Davis, Amanda Barabas, Rachel J. Mann, David F. LePage, Weihong Jiang, Mitchell L. Drumm, Thomas J. Kelley, Ronald A. Conlon, Craig A. Hodges *

Department of Genetics and Genome Sciences, Case Western Reserve University, Cleveland, Ohio, United States

ARTICLE INFO

Keywords:
Mouse model
Nonsense mutation
Organoids
W1282X

ABSTRACT

Background: People with cystic fibrosis carrying two nonsense alleles lack CFTR-specific treatment. Growing evidence supports the hypothesis that nonsense mutation identity affects therapeutic response, calling for mutation-specific CF models. We describe a novel *W1282X* mouse model and compare it to an existing *G542X* mouse.

Methods: The *W1282X* mouse was created using CRISPR/Cas9 to edit mouse *Cftr*. In this model, *Cftr* transcription was assessed using qRT-PCR and CFTR function was measured in the airway by nasal potential difference and in the intestine by short circuit current. Growth, survival, and intestinal motility were examined as well. Correction of *W1282X* CFTR was assessed pharmacologically and by gene-editing using a forskolin-induced swelling (FIS) assay in small intestine-derived organoids.

Results: Homozygous *W1282X* mice demonstrate decreased *Cftr* mRNA, little to no CFTR function, and reduced survival, growth, and intestinal motility. *W1282X* organoids treated with various combinations of pharmacologic correctors display a significantly different amount of CFTR function than that of organoids from *G542X* mice. Successful gene editing of *W1282X* to wildtype sequence in intestinal organoids was achieved leading to restoration of CFTR function.

Conclusions: The *W1282X* mouse model recapitulates common human manifestations of CF similar to other CFTR null mice. Despite the similarities between the congenic *W1282X* and *G542X* models, they differ meaningfully in their response to identical pharmacological treatments. This heterogeneity highlights the importance of studying therapeutics across genotypes.

1. Introduction

The development of CFTR modulators has changed the care for many people with cystic fibrosis (PwCF). These modulators increase CFTR protein function and reduce patient morbidity in the over 90% of PwCF carrying eligible mutations [1-3]. However, there are no safe and effective CFTR-directed therapies approved for nonsense mutations. Of the over 2000 reported mutations in CFTR, 7-8% are classified as nonsense mutations that generate premature termination codons (PTCs) [4,5]. Most transcripts containing PTCs are targeted for degradation via the nonsense-mediated decay (NMD) pathway [6]. PTC-containing transcripts that escape NMD yield truncated protein which may have little to no CFTR function [7]. Therapeutic strategies to treat nonsense mutations include PTC readthrough agents [8], NMD inhibition [9], suppressor tRNAs [10], and gene editing [11]. However, the diversity of nonsense mutations in CFTR may require different therapeutic strategies based on location or NMD sensitivity [12,13].

W1282X is the second most common *CFTR* nonsense mutation (1.2% of mutant *CFTR* alleles), the sixth most common *CFTR* mutation worldwide, and the most common mutation among Ashkenazi Jewish populations [5,14]. *W1282X* is a single base substitution mutation in exon 23 of the 27 exon-containing *CFTR* gene. Others have shown that the location of *W1282X* allows for the creation of a truncated protein, with 1281 amino acids versus the full length 1480 amino acid protein,

* Corresponding author at: Department of Genetics and Genome Sciences, Case Western Reserve University, Biomedical Research Building 725, 10900 Euclid Ave, Cleveland, OH 44106, USA.
E-mail address: craig.hodges@case.edu (C.A. Hodges).

https://doi.org/10.1016/j.jcf.2024.10.008
Received 7 June 2024; Received in revised form 28 August 2024; Accepted 20 October 2024

retaining channel activity in combination with CFTR modulators [15,16]. However, *W1282X*-mRNA is targeted by NMD limiting modulator effectiveness [17]. Various correction strategies have been explored in *W1282X*-expressing cells. An antisense oligonucleotide (ASO) toward NMD factor SMG1 increased expression and function in *W1282X*-expressing cell lines [18]. The combination of a SMG1 inhibitor and G418 readthrough allowed for almost 3% of WT function in a *W1282X*-expressing cell line [19]. Finally, Laselva and colleagues utilized several combinations of readthrough, NMD inhibition, and CFTR modulators in W1282X-expressing HBE cells to achieve various degrees of increase in both CFTR protein presence and function [20]. The effectiveness of these strategies for *W1282X* in vivo is unknown.

The development of a *W1282X* mouse model allows for existing and novel potential therapies including gene editing to be studied in vivo in a specific mutation context. While mouse models for other nonsense mutations exist (*G542X* [21], *R553X* [22]*),* it is hypothesized that these mice may differ in treatment response compared to W1282X. In human cells, any protein made from these PTCs in exon 12 are expected to produce protein truncation before or within the first nucleotide-binding domain (NBD) of CFTR [23]. Since *W1282X* occurs in the second NBD, it can yield a longer truncated protein that may respond differently to therapeutic strategies than the protein product of nonsense mutations earlier in the gene [15,24]. In this report, we generate the first *W1282X* animal model for CF. We show that the model is very similar in CF manifestations, mRNA expression and CFTR function to the *G542X* mouse model we previously published [21]. Surprisingly, small intestinal organoids derived from the *W1282X* mouse show dissimilar CFTR correction compared to *G542X* cells using various combinations of readthrough agents, a NMD inhibitor and CFTR modulators. This difference between these two mutations in response to PTC corrective compounds suggests different therapeutic strategies may be needed in patients with different nonsense mutations. The creation of another nonsense mutation in mice not only allows the comparison of different *Cftr* nonsense mutations but also allows for mutation-specific strategies to be tested in vivo.

2. Methods and Materials

Generation of the W1282X allele

To produce the *W1282X* mouse *Cftr* allele ($Cftr^{W1282X}$ or $Cftr^{em5Cwr}$), guide RNAs (gRNA) were designed in exon 23 of mouse *Cftr* based on proximity to target and off-target cutting analyses. Four gRNAs were tested in vitro using the Guide-it Complete Screening System kit (Takara Bio) for the ability to guide Cas9 nuclease activity to the given DNA sequence (Supplemental Figure 1; Supplemental Table 1). All the gRNAs tested drove cleavage to completion, so the guide which takes advantage of the *W1282X* mutation destroying the protospacer adjacent motif (PAM) site was selected for use in mice. One sgRNA (ATTCAGTGACCTTACAAGAA, 2.5-20ng/ul; IDT), a 120 bp single stranded oligonucleotide (ssODN) containing the *W1282X* mutation (2.5-20ng/ul; PNABio) (Supplemental Table 1) centered on the cut site and spCas9 protein (2.5-20ng/ul; PNABio) were injected into the pronucleus of C57BL/6J one-cell embryos. Embryos were then transferred into pseudo-pregnant females for gestation. Ear punches from the 36 progeny were sequenced using next generation sequencing. The region of interest was PCR amplified (~150 bp) with flanking primers that were tailed with a universal sequence. A secondary PCR amplification was then performed on the primary PCR product using a set of primers specific for the universal sequence and tailed with I5,I7 Illumina index and specific barcode sequences allowing for the sequencing of multiple samples at the same time. The mixture of barcoded PCR products was analyzed on an Illumina MiSeq instrument using a paired-end 300 base pair kit allowing for 25 million reads per run. Data were de-convoluted and variant analysis in comparison to the original sequence was performed using the OutKnocker software program [25]. 9 of 37 (24%) founder mice contained the desired W1282X mutation. One male founder mouse was bred to wild type mice to establish a line of W1282X heterozygous mutants congenic on C57BL/6J.

Mice

The *W1282X* mice were compared to a previously published *G542X* CF mouse model ($Cftr^{G542X}$ or $Cftr^{em3Cwr}$) which is also congenic on the C57BL/6J background [21]. Homozygous CF mice were created for both lines by breeding heterozygous females and males. Genotyping was completed using primer-probe sets described in Supplemental Table 1 and standard qPCR settings using a QuantStudio 5 (Thermo Fisher Scientific). Mice were allowed unrestricted access to acidified water and solid chow unless noted (Teklad S-2335 breeder diet (#7904); Envigo); kept on a 12-hour light, 12-hour dark cycle at a mean ambient temperature of 22°C; housed in standard ventilated polysulfone micro isolator cages with corncob bedding; and monitored daily.

In some experiments mice received polyethylene glycol (PEG)-3350 in their water to prevent intestinal blockage. Survival was monitored for up to 50 days of age in *W1282X* and WT mice not given PEG-3350. Female and male mice were used in each experiment. Data from the sexes was combined unless specified. Weight was assessed every five days for up to seven weeks of age. Mouse nasal-anal length was measured on euthanized six- to eight-week-old female and male mice. All animal use of procedures were approved by the Case Western Reserve University IACUC (approval #2014-0046).

Cftr Expression

Tissues were flash frozen and mechanically and chemically broken up by Trizol (Invitrogen). RNA was extracted by chloroform and reverse transcribed into cDNA using the qScript cDNA Synthesis kit (QuantaBio). RNA isolation from organoids grown densely on a 12-well plate was performed using the RNeasy mini kit (Qiagen) following manufacturer instructions. Real-time quantitative PCR (RT-qPCR) was performed on a StepOne Real-Time PCR System (Thermo Fisher Scientific). *Cftr* expression was assessed using a TaqMan assay with primers spanning exons 17 and 18 (Mm00445197; Applied Biosystems) normalized to β-actin as an endogenous control. Expression from each cDNA sample was run in duplicate. Expression values were averaged from all technical and biological replicates and normalized to WT expression for each tissue type.

Electrophysiology

Nasal potential difference (NPD) measurements were performed as previously described [26,27]. NPD was calculated from the change in electric potential across the nasal epithelium upon the addition of chloride-free HEPES buffered saline containing 10uM forskolin. The change in short circuit current (ΔI_{sc}) in $\mu A/cm^2$ across intestinal sections was performed as previously described [27] upon the administration of 100uM amiloride (Sigma A7410) to the apical side of the intestine and 10uM forskolin (Sigma F6886) to the basolateral side.

Intestinal Transit

Small intestinal transit was performed as described previously [28]. Adult mice were fasted overnight with free access to water. The next morning, rhodamine dextran in 1.5% methylcellulose saline (100uL of 25mg/mL; Sigma R9379) was administered by oral gavage. Mice were euthanized 40 minutes later and the GI tract was removed. The small intestine was divided into ten sections of equal length. The stomach, cecum, and intestinal sections were opened and flushed with 2 mL saline. GI tract contents were centrifuged (500 xG, 10 minutes) and 100uL of the resulting supernatant was placed in a black-bottomed 96-well plate (BRANDplates, Ref 781608). Fluorescence (excitation: 544nm;

emission: 590nm) was quantified using a fluorescent microplate reader (BMG Labtech's FLUOstar Omega). The distribution of fluorescent signal throughout the small intestine was used to calculate the geometric center of fluorescence (GCF). Specifically, the fraction of fluorescent signal in each section (relative to the total signal in the small intestine) and the intestinal segment number (1-10) were multiplied. Then, those ten numbers were added to yield GCF. A higher GCF indicates a faster intestinal transit time.

Compounds

G418 (Invivogen) was reconstituted in HEPES buffer to make an 80uM stock stored at 4°C. SMG1i (CFFT compound distribution program through Rosalind Franklin University of Medicine and Science) and 2,6-diaminopurine (DAP) (Sigma) was reconstituted in DMSO and stored at -20°C in 1 mM one time use aliquots. VX-445 and VX-661 (MedChemExpress) were reconstituted in DMSO and stored at -20°C in 3mM one time use aliquots. Forskolin (Sigma F6886) was reconstituted in 100% ethanol to make a 20mM working stock and stored at -20°C. All reagents for FIS were prepared immediately prior to use from stock.

Intestinal organoids

Small intestinal organoids were established from mice as described by others [29]. Briefly, mice were euthanized. The small intestine was removed, flushed with PBS, and cut longitudinally. Villi were gently removed by scraping. All PBS used lacked Mg^{2+} and Ca^{2+} (Corning). The intestine was cut into ~1 cm long sections and incubated under gentle rocking for 30 minutes in 30mL PBS containing 2mM EDTA. In a sterile tissue culture hood, the intestines were vortexed for 10 seconds, the supernatant was saved as a fraction, and the tube containing the intestine was refilled with 30 mL of PBS. This step was repeated to collect four fractions in total. Fractions were visualized and one highly enriched with crypts with minimal debris was selected and put through a 100 um cell strainer. Crypts were centrifuged at 250xG for five minutes. The supernatant was discarded. The pellet was resuspended in 100uL of a 1:1 mixture of Matrigel (Corning 356231) and Intesticult Organoid Growth Media (OGM; Stemcell Technologies 06005). The crypt solution was further diluted in 1:1 matrigel:OGM until the desired density was reached. In a 12-well plate (Corning Costar Cell Culture–Treated, Flat-Bottom microplates), 70uL of crypt suspension was plated into 5-7 domes per well and incubated at 37°C for 15 minutes. When domes were solidified 1mL of room temperature (RT) OGM was added to each well. Plates were stored at 37°C at 5% CO_2. Every 3-4 days, organoids were passaged by removing media, disrupting Matrigel domes with cold PBS, mechanically breaking up organoids, pelleting, resuspending in 1:1 Matrigel:OGM, and plating fresh domes.

Forskolin-Induced Swelling in Organoids

Forskolin-induced swelling (FIS) of murine small intestinal organoids was performed as described previously [7,30]. To minimize variability, multiple genotypes and drug treatments were evaluated simultaneously on the same plate. On average, each drug-genotype combination was assessed in three wells per plate. Additionally, each whole run (plating, drugging, swelling) was repeated independently on separate days. The data from different replicates and different days was averaged. During imaging, the Lionheart FX Automated Microscope (Bio Tek) plate chamber was kept at 37°C with an influx of 5% CO_2 and a filled humidity chamber. Corning Costar Cell Culture Treated, Flat-Bottom microplates (96 or 48 well) were imaged without lids. Organoids were passaged and plated into a 96-well plate with one 5uL dome (1:1 Matrigel:OGM) per well. Optimal density was 30-60 organoids per well. Wells were covered with 100uL of OGM ± drugs and incubated for 24 hours at 37°C with 5% CO2. Drug treatments included various combinations of 80uM G418, 1uM SMG1i, 25uM DAP, 3uM VX-661, and 3uM VX-445. Organoids were imaged for three hours with image capture every five minutes using the Lionheart FX. Immediately prior to imaging, 100uL of 1:1 DMEM:F12 + L-Glutamine, -HEPES, -phenol red (referred to herein as Opticlear; Gibco 21041025) containing forskolin was added to each well for a final forskolin concentration of 10uM. FIS over three hours was quantified per well by normalizing to the total organoid area at T = 0 using Gen5 software (BioTek). From these curves, the area under the curve (AUC) at T = 180 minutes was calculated.

Gene Edited Correction of W1282X Organoids

A 200 bp, single-stranded oligodeoxynucleotide (ssODN) containing WT sequence matching the *W1282X* mutation site was created (IDT, Supplemental Table 1). Organoids were grown in OGM containing 10uM Y-27632 (Tocris 1254) for 48 hours prior to treatment. Organoids were mechanically broken up and centrifuged at 200xG for five minutes. The supernatant was removed. The pellet was resuspended in 500uL of Accutase (Invitrogen) containing 10uM Y-27632, incubated for five minutes at 37°C with occasional vortexing, and then quenched with 500uL Advanced DMEM (Gibco). Cell density was estimated and cells were aliquoted so each reaction tube held ~150,000 cells. Cells were centrifuged at 300xG for five minutes. A RNP complex was prepared using the Lonza P3 Primary Cell 4D-Nucleofector X Kit S. P3 primary cell nucleofector solution, TrueCut Cas9 protein v2 (5uL/ug; Invitrogen), and sgRNA (100uM; Synthego) (CAGTGACCTTACAAGAATGA) were combined and incubated for 10 minutes at RT per manufacturer specifications. Cells were resuspended in P3 Primary Cell Nucleofector and Supplement 1 per manufacturer. To each cell suspension, RNP solution and either 25uM ssODN or vehicle were added. Suspensions were transferred to a 16-well Nucleovette strip) and electroporated in the Lonza 4D-Nucleofector X Unit (program DS-138). Electroporated cells were then combined with 70uL 1:1 Matrigel:OGM, plated on a 12-well plate (Corning CoStar Cell Culture Treated), and grown in OGM containing 10uM Y-27632 for three days. Gene-edited organoids were cultured for an additional week at which point primary selection was performed. Organoids were plated sparsely and 10uM forskolin was added to well media. Organoids displaying FIS were plucked from Matrigel using an extra-long P10 tip on a micropipette. Each swollen organoid was cultured in a separate well and allowed to form a homogenous population. Organoids underwent secondary FIS to measure percent of swelling and confirm homogeneity. Secondary FIS demonstrated one forskolin-sensitive homogenous population from which DNA was isolated and exon 23 of mouse *Cftr* was sequenced through Sanger sequencing. Sequence analysis utilized ICE (inference CRISPR Edits) software available through Synthego.

Statistics

Statistical analyses were performed using GraphPad Prism. Unless otherwise noted, data are shown as mean (*SD*), tests are two-sided, and the significance level was defined as 0.05. Normality was assessed graphically or by Q-Q plot of residuals. Weight and length were the only measures for which data from the sexes was not pooled and tests for females and males were conducted separately. Comparisons between groups for NPD, length, Isc, and GCF were done by Welch T-tests. Differences in weight were evaluated by a Welch T-test at each time point. Kaplan Meir survival curves were compared with the Gehan-Breslow-Wilcoxon test. FIS curves show standard error of the mean (SEM). FIS AUC were assessed with two-way ANOVAs assessing the interaction between drug treatment and genotype for both G418 and DAP groups. Raw G418 AUC data were not homoscedastic; therefore, the data was transformed by Y' = log (Y). The two-way ANOVA and post-hoc Tukey's multiple comparisons tests for the G418 AUC were conducted on the log transformed data. DAP AUC data were normal and homoscedastic and thus were untransformed prior to performance of a two-way ANOVA.

Post-hoc tests report adjusted P-values. For easier interpretation of the G418 ACU test statistics and graph, the summary data was back-transformed as Y'' = 10^(Y'). Because the G418 statistics were conducted on a log normal distribution, geometric mean and asymmetric 95% confidence intervals were reported. *Cftr* expression from gene edited and control organoids was compared by a Welch T-test.

3. Results

W1282X mouse recapitulates common CF manifestations

A comparison of human and mouse sequences and corresponding amino acids surrounding the CFTR *W1282X* mutation site is shown in Fig. 1. A mouse with *Cftr* containing *W1282X* was created by CRISPR/Cas9 gene editing (see methods). Homozygous *W1282X* mice (referred to as *W1282X*) were created by breeding heterozygous females and males. *Cftr* mRNA abundance was examined using RT-qPCR from the airway (lung and nasal epithelium), small intestine (duodenum, jejunum, and ileum), and kidney from wildtype (WT) and *W1282X* mice. *Cftr* transcript levels were significantly reduced in *W1282X* mice in all tissues compared to WT ranging from an average of 13-46% of corresponding WT expression (Fig. 1B). The reduction of *Cftr* mRNA in the homozygous *W1282X* was very similar to that of the *G542X*-containing CF mouse (Fig. 1B) [21]. We hypothesize this Cftr mRNA reduction

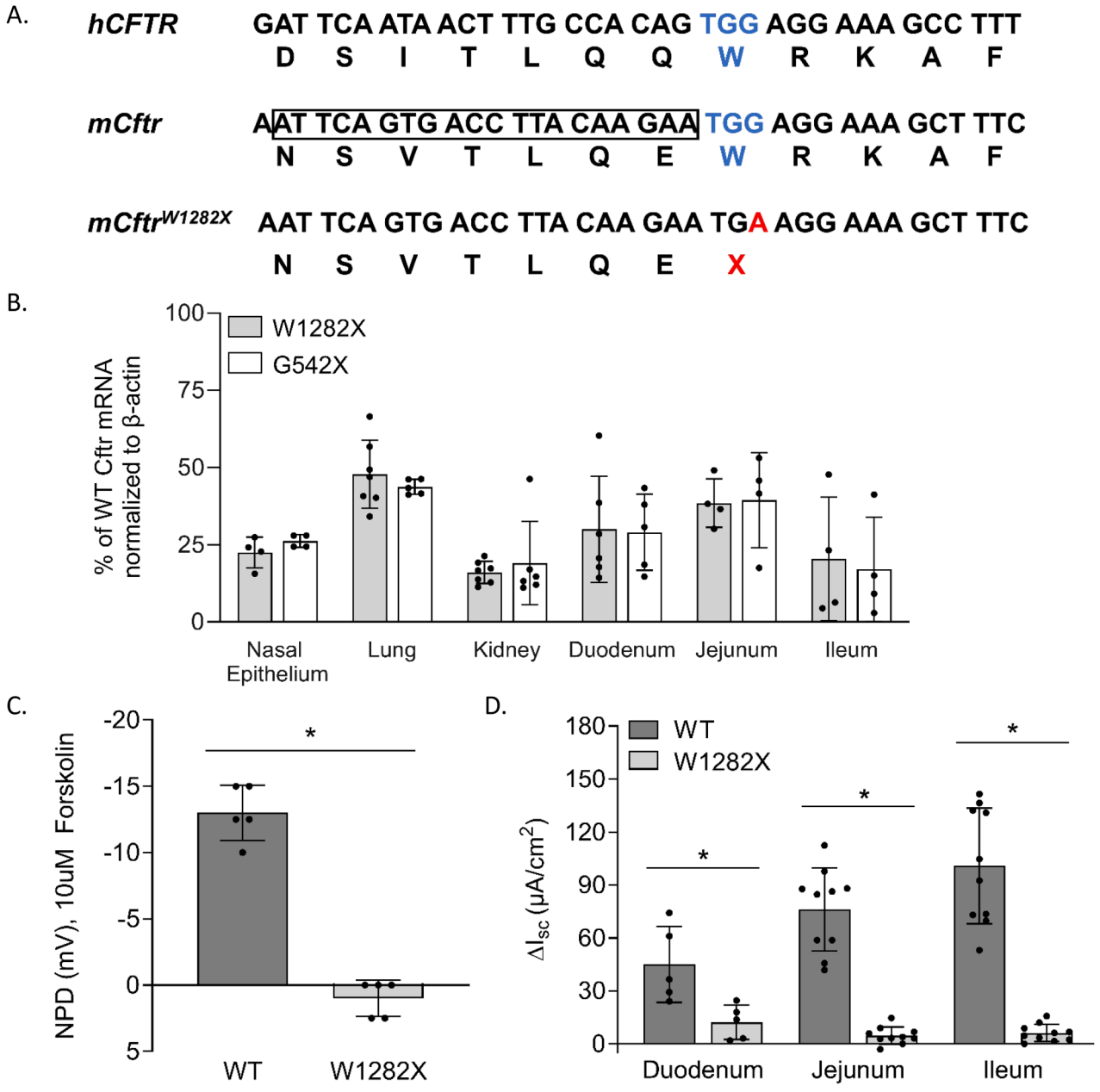

Fig. 1. *W1282X mouse* creation, expression, and function. (A) The DNA and amino acid sequences of human *CFTR (hCFTR),* mouse *Cftr (mCftr)*, and mouse *Cftr* with the *W1282X* mutation (*mCftr*^{W1282X}) surrounding the 1282nd codon. The desired mutation site is shown with the gRNA sequence (outlined) and the protospacer adjacent motif (PAM) sequence recognized by Cas9 (in blue). *Cftr*^{W1282X} DNA and amino acid sequence substitution change displayed in red. (B) *Cftr mRNA* expression in various tissues was measured by qRT-PCR from *W1282X* and *G542X* mice and normalized to *WT Cftr* expression ($n \geq 4$ mice/group). (C) CFTR function was assessed in the WT and *W1282X* mouse airway by nasal potential difference (NPD) in mV ($n = 5$, one measure per mouse, $^*P < .001$). (D) CFTR function was assessed in the mouse small intestine by the change in intestinal short circuit current (ΔI_{sc}) in uA/cm^2. One duodenum, two jejunum, and two ileum sections per mouse were used ($n = 5$ mice per genotype). Statistical tests were performed independently for each tissue section (*P ≤.02). Error bars represent *SD*.

relative to WT expression is due to NMD and that differences in NMD efficiency within different cell and tissue types account for the differences in *Cftr* expression across tissues [31].

To evaluate the effect of the *W1282X* mutation on CFTR function in the airway and the intestine, nasal potential difference (NPD) and intestinal short circuit current (I_{sc}) were observed in *W1282X* mice. The conductance of chloride anions across the nasal epithelium upon functional CFTR activation results in the NPD becoming more negative while the absence of functional CFTR results in a zero or positive NPD value [26,32]. *W1282X* homozygous mice demonstrated a significantly more positive NPD (in mV) upon CFTR activation than WT mice (1.00 (1.37), -13.00 (2.09), $P < .001$; Fig. 1C). CFTR function in the small intestine was measured by the change in short circuit current (ΔI_{sc}) upon CFTR activation. In each small intestinal section, *W1282X* mice displayed significantly reduced ΔI_{sc} (in $\mu A/cm^2$) compared to WT (Duo: 12.23 (9.70), 45.00 (21.57), $P = .02$; Jej: 4.63 (4.86), 67.76 (19.15), $P = .002$; Ileum: 31.45 (4.90), 100.6 (6.13), $P = .002$; Fig. 1D). Nasal and small intestinal electrophysiology results were consistent with other CF mouse models [21,27] indicative of complete loss of CFTR function in the *W1282X* mice.

Complete loss of CFTR in *W1282X* mice resulted in common CF manifestations observed in PwCF and CF mouse models such as reduced growth, intestinal obstruction, and slower intestinal transit time. *W1282X* and WT littermates were weighed every five days from 5-50

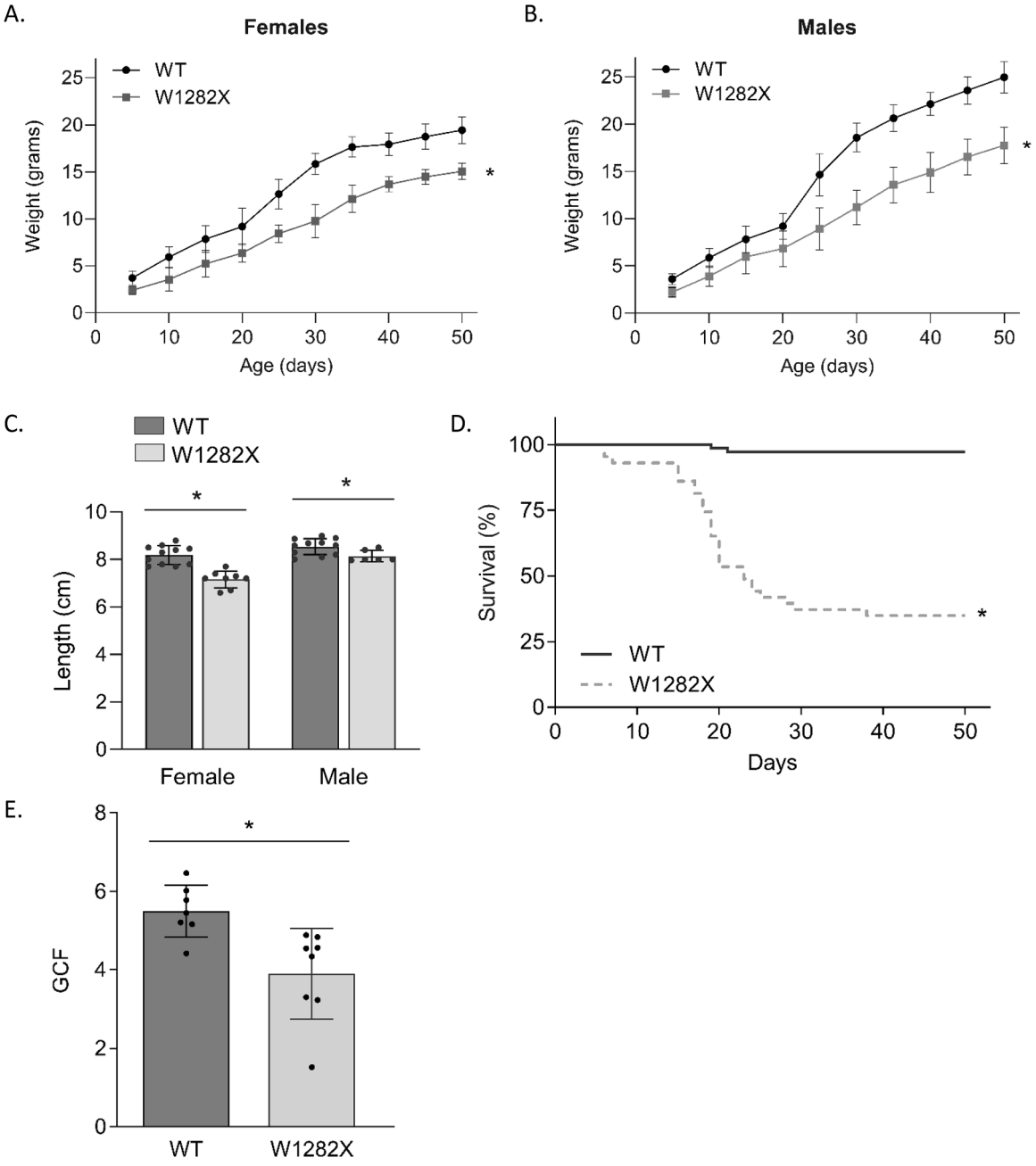

Fig. 2. W1282X mice recapitulate CF growth, survival, and dysbiosis phenotypes. (A) Female and (B) male *W1282X* and *WT* mice were weighed (in grams) every five days through 50 days of age. (Females: $n \geq 8$ per group per time, all $^*P \leq .001$; Males: $n \geq 7$ per group per time, $^*P \leq .002$). (C) The nose-to-anus length (in cm) was measured in female and male *W1282X* and *WT* mice 6-8 weeks of age (Female: $n \geq 8$ per genotype, $^*P < .001$; Male: $n \geq 6$ per genotype, $^*P = .015$). (D) Fifty-day survival of *W1282X* ($n = 43$; 34.8%) and *WT* ($n = 72$, 97.2%) mice was assessed ($^*P < .001$). (E) Gastrointestinal transit in adult *W1282X* ($n = 8$) and *WT* ($n = 7$) mice was assessed by the geometric center of fluorescence (GCF) (unitless) ($^*P = .007$). (A-E) Error bars represent *SD*.

days of age. Mean weights from *W1282X* mice were significantly smaller compared to WT at every time point in female and male mice ($P \leq .002$ for all; Fig. 2 A,B). *W1282X* mice also displayed reduced nose-to-anus length (in cm) at 6-8 weeks of age compared to WT littermates (F: 7.16 (0.36), 8.19 (0.40), $P < .001$; M: 8.14 (0.24), 8.54 (0.34), $P = .02$; Fig. 2C). *W1282X* mice have a significantly reduced fifty-day survival compared to WT littermates (34.8%, 97.2%, $P < .001$; Fig. 2D). The cause of death of *W128X* mice was confirmed by necropsy to be intestinal obstruction, which is rarely observed in WT mice. Intestinal transit studies measure the geometric center of fluorescence (GCF) to evaluate dysmotility. Higher GCF correlates to faster motility. *W1282X* mice have significantly lower GCF relative to WT littermates (3.90 (1.16), 5.50 (0.66); $P = .007$) indicative of delayed transit (Fig. 2E). The intestinal manifestations of the *W1282X* mice were identical to that of other CF mouse models [21,27,28,33].

W1282X and G542X models display different pharmacological correction

To interrogate the pharmacological restoration of *W1282X*-CFTR, intestinal primary cells from *W1282X* mice were cultured to establish small intestinal organoids. Activation of functional CFTR by forskolin stimulates the movement of anions, followed by water, into the organoid lumen resulting in forskolin-induced swelling (FIS) [30]. FIS of patient-derived rectal organoids treated with CFTR modulators is predictive of the clinical therapeutic response in the patient [34,35]. Small intestinal organoids derived from WT mice display robust FIS while *W1282X* organoids do not display FIS without correction (Fig. 3A).

Various pharmacological treatments of *W1282X*-CFTR had different degrees of restoring CFTR function in small intestinal organoids derived from *W1282X* mice. Initial treatments included G418, a readthrough agent that stimulates translational readthrough of premature termination codons; SMG1i, an NMD inhibitor; and VX-445 and VX-661 (elexacaftor and tezacaftor) CFTR correctors in the FDA-approved triple combination highly effective modulator therapy [1]. *W1282X* organoids were incubated with the following drug combinations for 24 hours, then treated with forskolin and imaged for three hours: G418 alone, G418+SMG1i, or a combination of G418+SMG1i+VX-445+VX-661. From the resulting images, the change in organoid area over time was calculated and normalized to the area at T = 0 corresponding to forskolin addition. Pretreatment of *W1282X* organoids with G418 alone resulted in minimal but reproducible FIS; moreover, pretreatment with SMG1i and G418 resulted in greater FIS than G418 alone while the greatest FIS was achieved by pretreatment with the full G418+SMG1i+VX-445+VX-661 combination (Fig. 3A, B).

There is growing evidence that different *CFTR* nonsense mutations respond differently to identical therapeutic strategies [36-40]. To investigate this phenomenon, small intestinal organoids derived from the novel *W1282X* mouse model and a previously published, *G542X* mouse model [1] were pretreated with either G418 alone, SMG1i alone, G418+SMG1i, or G418+SMG1i+VX-445+VX-661 for 24 hours, given forskolin, and immediately imaged for three hours. The area under the curve (AUC) was calculated from the resulting percent area increase curves. A two-way ANOVA was performed to analyze the effect of genotype and drug treatment on log-transformed AUC; drug treatment, genotype, and the interaction between the two had a significant effect (all $P \leq .01$) on AUC (Fig. 3C). *G542X* showed significantly greater AUC than *W1282X* in each treatment group when using post-hoc Tukey Tests. A possible explanation could be that the *G542X* allele produces more *Cftr* mRNA at baseline or upon pharmacological treatment. mRNA was collected from treated organoids and *Cftr* mRNA was assessed by qRT-PCR. There was no difference in *Cftr* mRNA between *W1282X* and *G542X* organoids regardless of the treatment group (Fig. 3D). While pretreatment with SMG1i alone did result in an expected robust increase in *Cftr* mRNA regardless of mutation similar to work done in patient derived intestinal organoids (PDOs)[41], this did not lead to any detectable CFTR function by FIS during the three hours of observation (Fig. 3C,D).

Another potential therapeutic treatment of PTC CF organoids included 2,6-diaminopurine (DAP) which is a compound that exhibits PTC readthrough ability specifically for UGA nonsense mutations [42]. DAP interferes with a tRNA-specific 2'-O-methyltransferase, which modifies a cytosine in $tRNA^{Trp}$, leading to the recognition of the UGA stop codon and pairing with the near-cognate $tRNA^{Trp}$. Tryptophan is the only amino acid found to be inserted at the PTC after treatment with DAP [42]. Both *G542X* and *W1282X* are UGA nonsense mutations but we hypothesize that DAP treatment would lead to a greater restoration of CFTR function in *W1282X* containing cells given that tryptophan is the naturally occurring amino acid at that position in the CFTR. Similar to what was done in the above experiments, *W1282X* and *G542X* mouse organoids were pretreated with combinations of DAP and CFTR modulators. Robust FIS was observed in both populations of organoids but CFTR activity was significantly greater in *W1282X* organoids (Fig. 3E,F).

Gene editing of W1282X restores Cftr expression and function

To assess the ability to correct the *W1282X* mutation by gene editing and its subsequent effect on CFTR function, we utilized organoids derived from a homozygous *W1282X* mouse. Fig. 4A summarizes the gene editing procedure including the digestion of organoids to single cells, the introduction of gRNA-Cas9 RNP and a WT-ssODN via electroporation, recovery and reforming of organoids, primary selection by FIS, and expansion of gene edited (GE) clonal populations. This method of CFTR correction in organoids is similar to a procedure described by others [43,44] but instead of using selectable markers or fluorescent tags, FIS in brightfield was used as an indicator for CFTR correction. FIS was observed in ~25% of organoids electroporated with all three components for gene editing while organoids treated with Cas9 alone or Cas9 and gRNA displayed little to no FIS (Fig. 4B). The resulting clonal population was derived from a single swollen organoid isolated at primary selection by FIS. The gene edited clonal population demonstrated widespread, robust FIS within one hour similarly to WT controls (Fig 5A, B). Sequencing revealed that no unedited alleles remained in the GE clone; there was one allele with WT sequence and one allele with a 17 base pair deletion around the site of the guide (Supplemental Figure 2). *Cftr* expression was measured in unedited *W1282X* organoids and the GE clonal organoids which had >50% of WT *Cftr* expression. *Cftr* expression was significantly higher in the GE clonal organoids compared to unedited W1282X (Control: 12.99% (3.38), GE Clone: 70.40% (10.88), $P < .001$; Fig 5C). These data suggest that this *W1282X* CF mouse model will also be useful in assessing gene editing success in vivo.

4. Discussion

Despite CF being a monogenic disease, substantial genetic and pathophysiological heterogeneity exists amongst PwCF. Over 2000 *CFTR* mutations have been identified in CFTR with many associated with severe disease manifestations and others associated with milder disease. Even amongst PwCF homozygous for the most common CFTR mutation, F508del, disease severity can differ widely. This is attributed to both genetic variation outside of CFTR and the environment [45]. There is also heterogeneity in treatment responsiveness among mutations eligible for modulator use [46]. Even among only CFTR nonsense mutations, there is meaningful heterogeneity. For example, there are over 170 CFTR nonsense mutations with varied locations throughout the gene causing different susceptibility to NMD [24]. Additionally, nonsense mutations create multiple types of PTCs (amber, ochre, or opal). Furthermore, different PTCs may be differentially responsive to the same therapeutic approach. For example, several studies have shown that CFTR PTCs in human bronchial epithelial cells (HBEs) and PDOs had significantly different CFTR restoration depending on the pharmacologic correctors used [41,47]. Interestingly, these studies and others have shown some of this CFTR restoration variability may also be due to

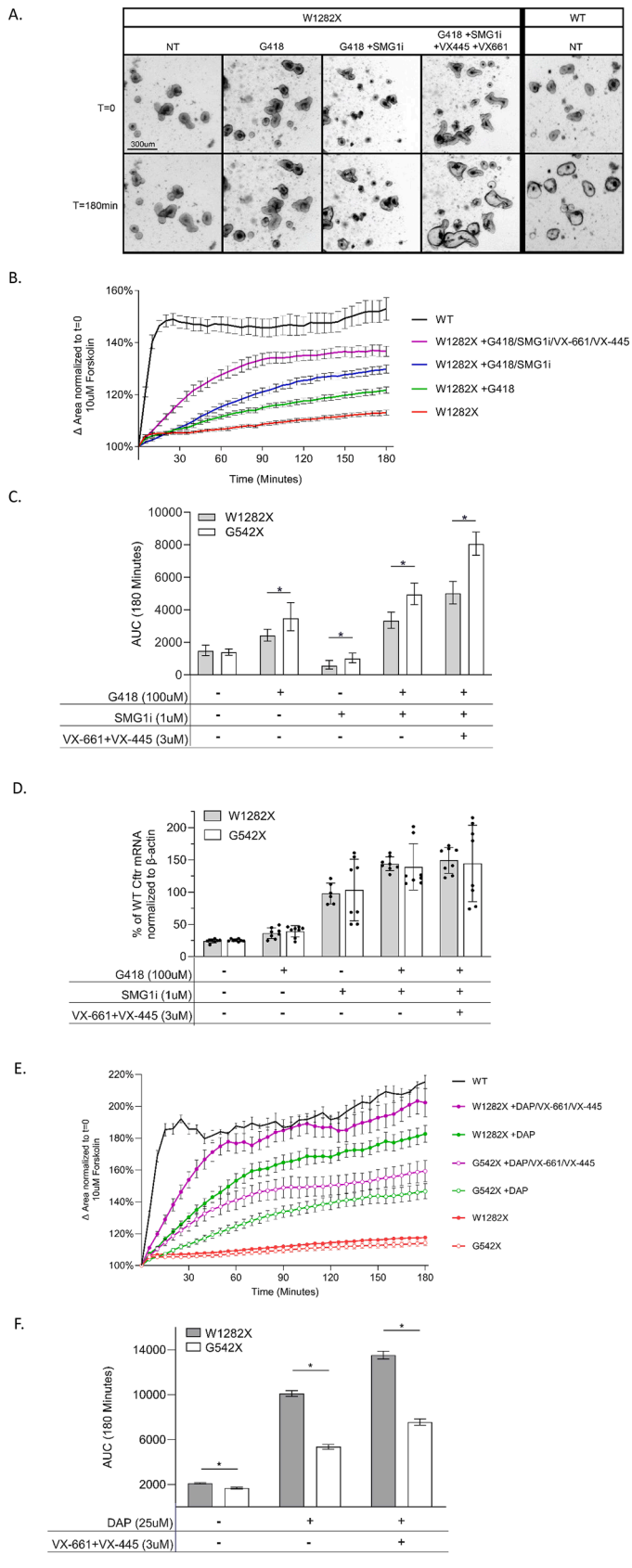

(caption on next column)

Fig. 3. Pharmacologic correction of W1282X and G542X in mouse intestinal organoids. *W1282X* and *WT* small intestinal mouse organoids were treated with the specified treatment conditions for 24 hours prior to forskolin-induced swelling (FIS). (A-D) Treatments include G418, SMG1i, VX-661 and VX-445. (E-F) Treatments include DAP, VX-661 and VX-445. (A) Representative images of *W1282X* and WT organoids at T = 0 and T = 180 minutes of FIS. NT = 'no treatment'. (B,E) Change in the organoid area over three hours normalized to the area at T = 0m was captured for the indicated treatment conditions. Error bars represent SEM. (C,F) The area under the curve (AUC) at 180 minutes for *G542X* and *W1282X* organoids under various treatments. ($n \geq 7$ replicates; $^*P \leq .002$). (D) *mCftr mRNA* expression in *W1282X* and *WT* organoids upon the specified treatment conditions measured by qRT-PCR normalized to expression from untreated WT organoids. Error bars represent SD.

differences inherent in the patient donor of the cells [22,41,47,48]. Acknowledging and understanding these sources of heterogeneity will be important in identifying successful cures for *CFTR* nonsense mutations. The creation of a *W1282X* mouse model, described in this manuscript, marks the first *W1282X*-specific animal model which can be used to examine CFTR functional restoration by small molecules and gene editing. Using this novel model, we compared CF manifestations and CFTR functional restoration amongst different nonsense mutations.

The *W1282X* mouse recapitulates many common human CF manifestations including reduced growth, poor survival due to intestinal obstruction, and delayed intestinal transit (Fig. 2). Additionally, the *W1282X* mouse displayed a fraction of WT-level *Cftr* mRNA across tissues, which may be due to degradation of nonsense transcripts by NMD, as well as an absence of functional CFTR in mouse airway and GI tissues (Fig. 1). The *W1282X* mouse growth, intestinal motility, survival, mRNA expression, and CFTR functional phenotypes were nearly identical to those of the congenic *G542X* mouse [21]. Interestingly, we did observe important differences between organoids derived from *W1282X* and *G542X* when attempting to restore CFTR function using various combinations of translational readthrough induction, nonsense mediated decay inhibition and CFTR modulators. Using the sensitive forskolin induced swelling assay in intestinal organoids, we observed that while CFTR function could be restored in *W1282X* organoids the restoration was substantially reduced compared to restoration in G542X organoids when using G418 but increased compared to restoration in G542X organoids when using DAP (Fig. 3). This difference in CFTR restoration between genotypes is not explained by differential *Cftr* expression or NMD efficiency. Expression of *Cftr* mRNA was highly similar between *G542X* and *W1282X* organoids treated with identical control or pharmacological treatments; additionally, *Cftr* mRNA expression was rescued equally in each genotype upon NMD inhibition (Fig. 3D). We hypothesize that the difference in CFTR restoration observed between *W1282X* and *G542X* organoids stem from differences in translational readthrough induction.

Similarities between *W1282X* and *G542X* include causing UGA "opal" PTCs, yielding transcripts subject to NMD, and occurring in CFTR nucleotide-binding domains (NBDs). The most notable difference between the two mutations is location. *G542X* is in exon 12 corresponding to NBD1 while *W1282X* is in exon 23 corresponding to NBD2; therefore, *W1282X* CFTR protein could be a much longer truncated protein than *G542X*. Indeed, CFTR modulators have been reported to increase the function of truncated *W1282X* CFTR when overexpressed in FRT cells [15]; however, results in human nasal epithelial cells (HNEs) and HBEs carrying the *W1282X* mutation have shown no restoration of function without translational readthrough and/or NMD inhibition [17,20,39]. It is well known that PTC identity affects translational termination efficiency. Additionally, the sequence adjacent to the nonsense mutation affects basal translational readthrough efficiency and likely antibiotic induced readthrough [49,50]. The nucleotide immediately downstream of the stop codon (location +4 if the start of the stop codon is +1) has the largest effect on readthrough efficiency [49]. The identities of nucleotides in the 3' positions +4 to +9 and 5' positions -1 and -2 also affect

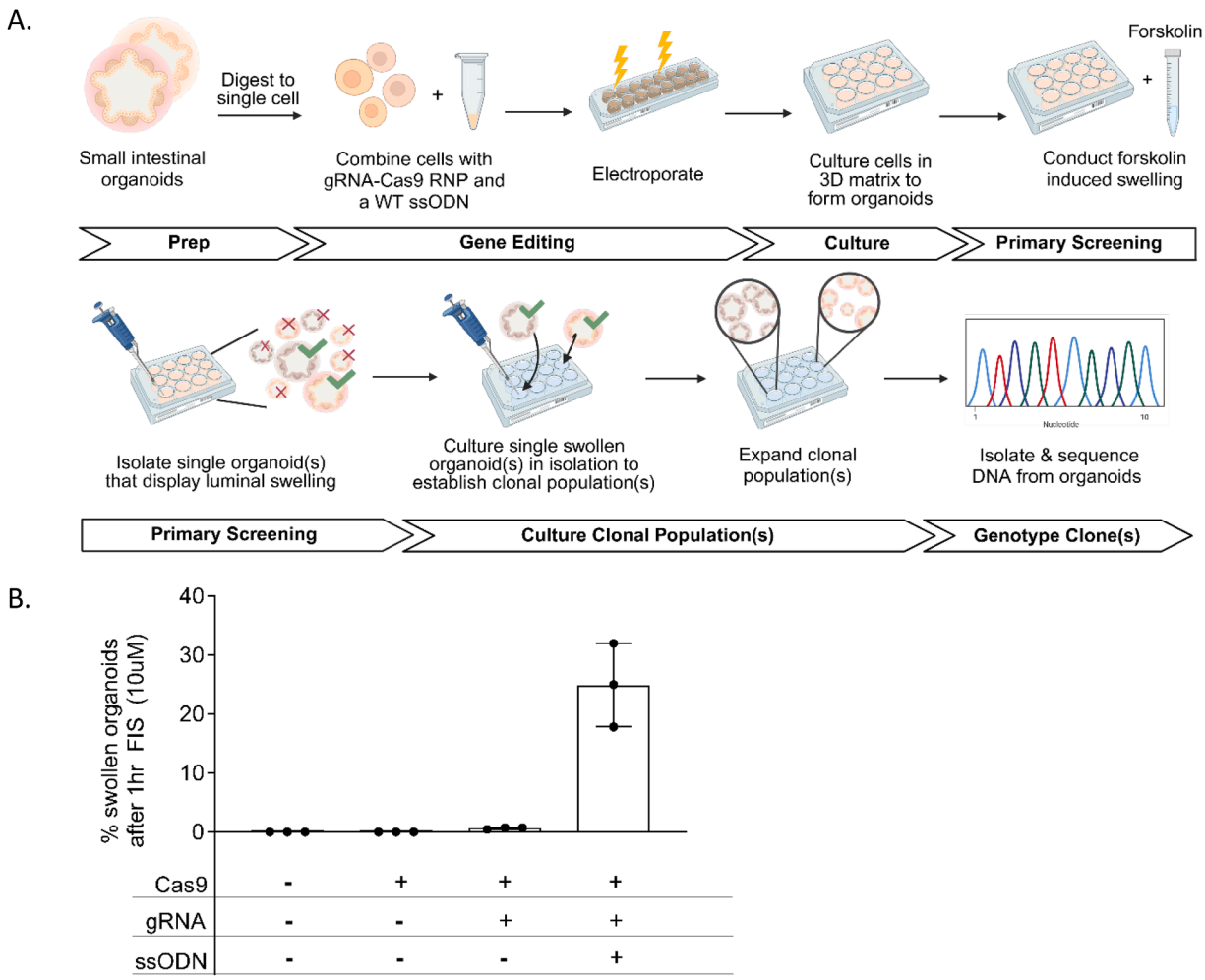

Fig. 4. Gene editing W1282X small intestinal organoids (A) A visual summary of the gene editing protocol used in mouse intestinal organoids. *W1282X* organoids were digested; gene-edited with gRNA-Cas9 ribonucleoprotein (RNP) and a WT single stranded deoxynucleotide (ssODN); electroporated; and cultured. Organoids demonstrating FIS in primary selection were isolated to establish a clonal population. (B) During primary selection after 1 hour of FIS, ~25% of W1282X organoids treated with all gene-editing components displayed swelling. Organoids electroporated with no components, Cas9 alone or Cas9 and gRNA displayed few to no swelled organoids.

readthrough efficiency with 5' sequence effects being the weakest [49, 50]. The -2 through the +6 nucleotide positions are the most well-described modulators of readthrough efficiency [51,52]. Thus, differences in mouse and human sequence surrounding a stop codon may limit the translatability of readthrough studies conducted in mice. Importantly, the human and mouse *W1282X* sequences are identical at the -2 and +1 through +9 positions (Fig. 1A) thus minimizing this potential limitation. This sequence may also affect the identity of the amino acid inserted at the PTC site during translational readthrough which is known to rarely be the amino acid present in WT CFTR when using aminoglycosides [53]. Interestingly, Xue et al., showed that G542X is less likely to incorporate the wild-type amino acid than W1282X. In our studies, we find that G542X had greater CFTR restoration than W1282X when treated with G418 alone, G418+SMG1i, and G418+SMG1i+VX-445+VX-661 which may be due to sequence context. This difference is supported by work from Valley et al., which found reduced CFTR restoration upon treatment with G418 alone and G418+SMG1i in *W1282X* isogenic cell models compared to *G542X* [19]. In human cells, Laselva and colleagues also observed significant CFTR restoration in *W1282X* HNEs treated with G418, SMG1i and CFTR modulators but comparison with *G542X* HNEs was not completed [20]. In PDOs, both *G542X* and *W1282X* were treated with similar compounds (readthrough agent, a NMD inhibitor and modulators) and both mutations showed robust CFTR restoration but donor response variability in CFTR restoration made mutation comparison difficult with *W1282X* PDOs having a wide range of restoration [41]. Similar to our findings, Leroy et al., utilized DAP as a readthrough agent on PDOs and observed a greater response in *W1282X* than *G542X* organoids [22].

Translational readthrough of PTCs occurs rarely (<0.1%) under normal conditions in mammalian cells [54]. Increasing translational readthrough of PTCs has been a major area of focus for potential therapies for PTCs in CF and other genetic disorders originating from PTCs. Aminoglycosides, a family of antibiotics which includes G418 and gentamicin, were one of the first translational readthrough compounds identified that displayed some successful PTC readthrough in CF [55]. However, ototoxicity and nephrotoxicity are major complications with using aminoglycosides [56]. A synthetic aminoglycoside, ELX-02, with less toxicity has shown efficacy in PDOs [57] and is currently in phase 2 clinical trials in CF in combination with a CFTR modulator. Ataluren, a potential translational readthrough compound identified in a high-throughput screen, has a long history of conflicting reports on its success in producing readthrough of *CFTR* PTCs [48] but has been approved for use in Europe for nonsense mutations in Duchenne muscular dystrophy. In addition, Ataluren derivatives have shown improved readthrough in vitro and tolerability in mice [58]. Other compounds with less toxicity than aminoglycosides such as escin, a natural product, and amlexanox, a drug used for canker sores, have also been identified as potential PTC readthrough agents [59,60] but have

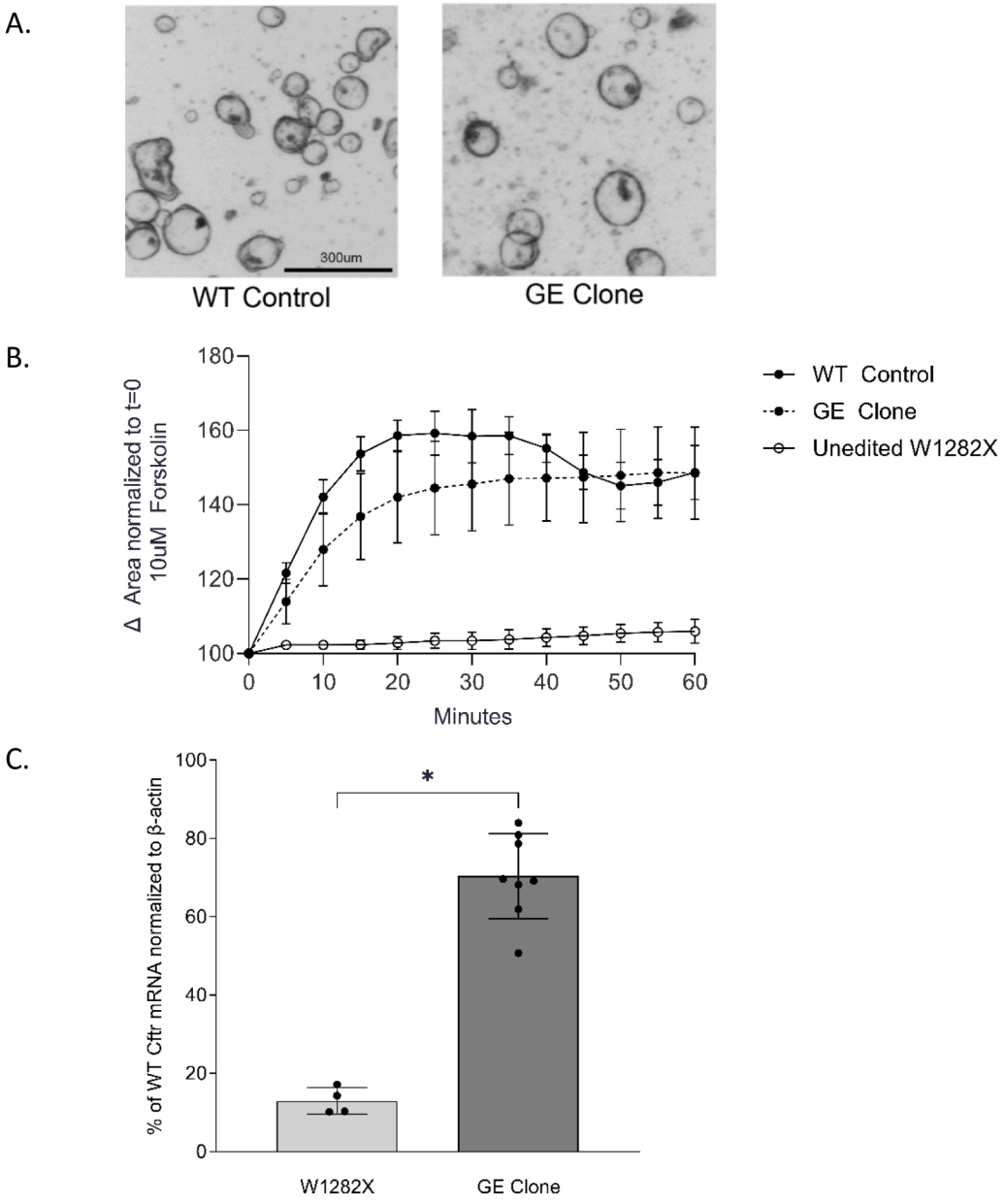

Fig. 5. Correction of *W1282X* allele in organoids using CRISPR-Cas9 editing. (A) Representative images of a gene-edited (GE) clonal organoid population and a WT control one hour after treatment with 10uM forskolin. (B) Change in the organoid area over one hour normalized to the area at T = 0 of a GE clonal population, a WT control and unedited W1282X control treated with 10uM forskolin. Each group underwent at least two independent FIS experiments on different days with three technical replicates per group (n≥6 data points) (C) Expression of *Cftr mRNA* from unedited W1282X organoids and a GE clonal organoid population normalized to the expression from WT organoids measured by qRT-PCR. Averages of multiple technical replicates are shown. Error bars represent SD. (*$P < .001$)

not displayed efficacy in *G542X* mouse-derived small intestinal organoids [7]. The type of PTC may affect efficacy for certain translational readthrough agents. For instance, clitocine, a nucleoside analog, displays varied success of PTC readthrough based on codon identity with the highest readthrough of codon UAA and less readthrough of UGA and UAG respectively; however no in vivo success has been published [61]. Similarly, DAP, a compound with low toxicity shows a preference of readthrough of the UGA PTC and has recently been tested in an *R553X* animal model and PDOs with some success [22,42] which our data in this manuscript support. The *W1282X* mouse model will be a useful tool for testing both short and long term in vivo CFTR correction with some of these less toxic translational readthrough compounds like DAP.

Given the potentially heterogeneous pharmacologic correction of nonsense mutations in CFTR, gene editing is another nonsense mutation correction strategy. We show in vitro using traditional CRISPR-Cas9 components that editing just one copy of *W1282X* to the wildtype sequence restores CFTR function fully in mouse-derived intestinal organoids (Fig. 5 and Supplemental Figure 2). Recent advances in gene editing have led to FDA approval of several gene therapies for genetic disorders [62,63]. Gene editing in CF will be complicated because of its multiorgan disease manifestations. However, as both gene editors and delivery agents improve gene editing for CFTR mutations may become a reality [64]. Animal models, like the *W1282X* model described in this manuscript, will assist in examining the success of these editors and delivery agents needed for a gene-editing cure. While sequence differences between human and mouse will generally require different gRNA sequence, a strength of using mice carrying mutations congenic on an inbred background is that the environment and genetic components are fixed eliminating these factors as contributing to variability in gene editing success.

In summary, the *W1282X* mouse model described in this manuscript displays similar disease manifestations as other CF mouse models that have little to no CFTR function. Reduced *Cftr* mRNA and CFTR function in this model was similar to that of the *G542X* mouse model. Interestingly, the ability to restore CFTR function with translational readthrough, NMD inhibition, and CFTR modulators in the *W1282X* model was substantially different compared to the *G542X* model depending on the specific agents used. The heterogeneous CFTR functional restoration witnessed in these congenic nonsense mutation models highlights the need to better understand the action of translational readthrough agents on nonsense mutations as well as the potential contribution of adjacent sequence. Regardless of the underlying mechanisms, the different correction phenotypes between *W1282X* and *G542X* illustrate that different nonsense mutations may require different therapeutic strategies to yield clinically relevant CFTR correction. To our knowledge, this is the first *W1282X*-specific animal model with *Cftr* under endogenous regulatory control. This model is a powerful tool with which to study CFTR biology and therapeutic strategies (pharmacologic and gene editing) in a *W1282X*-specific context both in vitro and in vivo. Furthermore, our functional studies using mouse-derived small intestinal organoids contribute to the field's understanding of *Cftr* nonsense mutation heterogeneity. Our work further supports a precision medicine approach to treating CF caused by nonsense mutations.

CRediT authorship contribution statement

Margaret Michicich: Conceptualization, Methodology, Validation, Formal analysis, Investigation, Writing – original draft, Writing – review & editing. **Zachary Traylor:** Methodology, Validation, Formal analysis, Investigation, Writing – review & editing. **Caitlan McCoy:** Methodology, Validation, Formal analysis, Investigation, Writing – review & editing. **Dana M. Valerio:** Formal analysis, Investigation, Writing – review & editing. **Alma Wilson:** Investigation, Resources, Writing – review & editing. **Molly Schneider:** Investigation, Resources, Writing – review & editing. **Sakeena Davis:** Investigation, Resources, Writing – review & editing. **Amanda Barabas:** Investigation, Resources, Writing – review & editing. **Rachel J. Mann:** Methodology, Resources, Writing – review & editing. **David F. LePage:** Methodology, Resources, Writing – review & editing. **Weihong Jiang:** Methodology, Resources, Writing – review & editing. **Mitchell L. Drumm:** Resources, Supervision, Writing – review & editing. **Thomas J. Kelley:** Resources, Supervision, Writing – review & editing. **Ronald A. Conlon:** Methodology, Resources, Supervision, Writing – review & editing. **Craig A. Hodges:** Conceptualization, Methodology, Formal analysis, Investigation, Writing – original draft, Writing – review & editing, Supervision, Funding acquisition.

Declaration of competing interest

Authors report no conflicts of interest.

Acknowledgements

We would like to thank Michael Wilson and Sara Mansbach for their assistance in the short circuit current measurements. Fig. 4A and Supplemental Figure 2 was created using Biorender.com.

Funding

This work was supported by grants from Emily's Entourage [Emily's Entourage, 2021]; the Cystic Fibrosis Foundation [Hodges19R1, Hodges23R1]; the National Institutes of Health [NIH- F31HL166193, 2022 and T32GM135081, 2019].

Supplementary materials

Supplementary material associated with this article can be found, in the online version, at doi:10.1016/j.jcf.2024.10.008.

References

[1] Middleton PG, et al. Elexacaftor-Tezacaftor-Ivacaftor for Cystic Fibrosis with a Single Phe508del Allele. N Engl J Med 2019;381(19):1809–19.
[2] Ramsey BW, et al. A CFTR potentiator in patients with cystic fibrosis and the G551D mutation. N Engl J Med 2011;365(18):1663–72.
[3] Wainwright CE, et al. Lumacaftor-Ivacaftor in Patients with Cystic Fibrosis Homozygous for Phe508del CFTR. N Engl J Med 2015;373(3):220–31.
[4] Cystic Fibrosis Mutation Database (CFTR1); available at http://www.genet.sickkids.on.ca/cftr/Home.html.
[5] The Clinical and Functional TRanslation of CFTR (CFTR2); available at http:/cftr2.org.
[6] Lindeboom RGH, et al. The impact of nonsense-mediated mRNA decay on genetic disease, gene editing and cancer immunotherapy. Nat Genet 2019;51(11):1645–51.
[7] McHugh DR, Cotton CU, Hodges CA. Synergy between Readthrough and Nonsense Mediated Decay Inhibition in a Murine Model of Cystic Fibrosis Nonsense Mutations. Int J Mol Sci 2020;22(1).
[8] Xue X, et al. Synthetic aminoglycosides efficiently suppress cystic fibrosis transmembrane conductance regulator nonsense mutations and are enhanced by ivacaftor. Am J Respir Cell Mol Biol 2014;50(4):805–16.
[9] Linde L, et al. Nonsense-mediated mRNA decay affects nonsense transcript levels and governs response of cystic fibrosis patients to gentamicin. J Clin Invest 2007;117(3):683–92.
[10] Porter JJ, Heil CS, Lueck JD. Therapeutic promise of engineered nonsense suppressor tRNAs. Wiley Interdiscip Rev RNA 2021;12(4):e1641.
[11] Hodges CA, Conlon RA. Delivering on the promise of gene editing for cystic fibrosis. Genes Dis 2019;6(2):97–108.
[12] Popp MW, Maquat LE. Leveraging Rules of Nonsense-Mediated mRNA Decay for Genome Engineering and Personalized Medicine. Cell 2016;165(6):1319–22.
[13] Supek F, Lehner B, Lindeboom RGH. To NMD or Not To NMD: Nonsense-Mediated mRNA Decay in Cancer and Other Genetic Diseases. Trends Genet 2020.
[14] Shoshani T, et al. Association of a nonsense mutation (W1282X), the most common mutation in the Ashkenazi Jewish cystic fibrosis patients in Israel, with presentation of severe disease. Am J Hum Genet 1992;50(1):222–8.
[15] Haggie PM, et al. Correctors and Potentiators Rescue Function of the Truncated W1282X-Cystic Fibrosis Transmembrane Regulator (CFTR) Translation Product. J Biol Chem 2017;292(3):771–85.
[16] Wang W, et al. Robust Stimulation of W1282X-CFTR Channel Activity by a Combination of Allosteric Modulators. PLoS One 2016;11(3):e0152232.
[17] Aksit MA, et al. Decreased mRNA and protein stability of W1282X limits response to modulator therapy. J Cyst Fibros 2019;18(5):606–13.
[18] Keenan MM, et al. Nonsense-mediated RNA Decay Pathway Inhibition Restores Expression and Function of W1282X CFTR. Am J Respir Cell Mol Biol 2019;61(3):290–300.
[19] Valley HC, et al. Isogenic cell models of cystic fibrosis-causing variants in natively expressing pulmonary epithelial cells. J Cyst Fibros 2019;18(4):476–83.
[20] Laselva O, et al. Functional rescue of c.3846G>A (W1282X) in patient-derived nasal cultures achieved by inhibition of nonsense mediated decay and protein modulators with complementary mechanisms of action. J Cyst Fibros 2020;19(5):717–27.
[21] McHugh DR, et al. A G542X cystic fibrosis mouse model for examining nonsense mutation directed therapies. PLoS One 2018;13(6):e0199573.
[22] Leroy C, et al. Use of 2,6-diaminopurine as a potent suppressor of UGA premature stop codons in cystic fibrosis. Mol Ther 2023;31(4):970–85.
[23] Fang X, Yeh JT, Hwang TC. Pharmacological Responses of the G542X-CFTR to CFTR Modulators. Front Mol Biosci 2022;9:921680.
[24] Sharma N, et al. Capitalizing on the heterogeneous effects of CFTR nonsense and frameshift variants to inform therapeutic strategy for cystic fibrosis. PLoS Genet 2018;14(11):e1007723.
[25] Schmid-Burgk JL, et al. OutKnocker: a web tool for rapid and simple genotyping of designer nuclease edited cell lines. Genome Res 2014;24(10):1719–23.
[26] Brady KG, Kelley TJ, Drumm ML. Examining basal chloride transport using the nasal potential difference response in a murine model. Am J Physiol Lung Cell Mol Physiol 2001;281(5):L1173–9.
[27] Hodges CA, et al. Generation of a conditional null allele for Cftr in mice. Genesis 2008;46(10):546–52.
[28] Vitko M, et al. A novel guluronate oligomer improves intestinal transit and survival in cystic fibrosis mice. J Cyst Fibros 2016;15(6):745–51.
[29] Sato T, et al. Single Lgr5 stem cells build crypt-villus structures in vitro without a mesenchymal niche. Nature 2009;459(7244):262–5.
[30] Dekkers JF, et al. A functional CFTR assay using primary cystic fibrosis intestinal organoids. Nat Med 2013;19(7):939–45.
[31] Rivas MA, et al. Human genomics. Effect of predicted protein-truncating genetic variants on the human transcriptome. Science 2015;348(6235):666–9.
[32] Kelley TJ, et al. In vivo activation of the cystic fibrosis transmembrane conductance regulator mutant deltaF508 in murine nasal epithelium. Proc Natl Acad Sci U S A 1997;94(6):2604–8.
[33] Hodges CA, et al. Cystic fibrosis growth retardation is not correlated with loss of Cftr in the intestinal epithelium. Am J Physiol Gastrointest Liver Physiol 2011;301(3):G528–36.
[34] Boj SF, et al. Forskolin-induced Swelling in Intestinal Organoids: An In Vitro Assay for Assessing Drug Response in Cystic Fibrosis Patients. J Vis Exp 2017;(120).

[35] Dekkers JF, et al. Characterizing responses to CFTR-modulating drugs using rectal organoids derived from subjects with cystic fibrosis. Sci Transl Med 2016;8(344):344ra84.
[36] Liang F, et al. High-Throughput Screening for Readthrough Modulators of CFTR PTC Mutations. SLAS Technol 2017;22(3):315–24.
[37] Manuvakhova M, Keeling K, Bedwell DM. Aminoglycoside antibiotics mediate context-dependent suppression of termination codons in a mammalian translation system. RNA 2000;6(7):1044–55.
[38] Pranke IM, et al. The U UGA C sequence provides a favorable context to ELX-02 induced CFTR readthrough. J Cyst Fibros 2023;22(3):560–3.
[39] Venturini A, et al. Comprehensive Analysis of Combinatorial Pharmacological Treatments to Correct Nonsense Mutations in the CFTR Gene. Int J Mol Sci 2021;22(21).
[40] Yu H, et al. Comparison of read-through effects of aminoglycosides and PTC124 on rescuing nonsense mutations of HERG gene associated with long QT syndrome. Int J Mol Med 2014;33(3):729–35.
[41] de Poel E, et al. Functional Restoration of CFTR Nonsense Mutations in Intestinal Organoids. J Cyst Fibros 2022;21(2):246–53.
[42] Trzaska C, et al. 2,6-Diaminopurine as a highly potent corrector of UGA nonsense mutations. Nat Commun 2020;11(1):1509.
[43] Artegiani B, et al. Fast and efficient generation of knock-in human organoids using homology-independent CRISPR-Cas9 precision genome editing. Nat Cell Biol 2020;22(3):321–31.
[44] Schwank G, et al. Functional repair of CFTR by CRISPR/Cas9 in intestinal stem cell organoids of cystic fibrosis patients. Cell Stem Cell 2013;13(6):653–8.
[45] Sharma N, Cutting GR. The genetics and genomics of cystic fibrosis. J Cyst Fibros 2020;19 Suppl 1(Suppl 1):S5–9.
[46] Clancy JP, et al. CFTR modulator theratyping: Current status, gaps and future directions. J Cyst Fibros 2019;18(1):22–34.
[47] Mutyam V, et al. Novel Correctors and Potentiators Enhance Translational Readthrough in CFTR Nonsense Mutations. Am J Respir Cell Mol Biol 2021;64(5):604–16.
[48] Spelier S, et al. Readthrough compounds for nonsense mutations: bridging the translational gap. Trends Mol Med 2023;29(4):297–314.
[49] Dabrowski M, Bukowy-Bieryllo Z, Zietkiewicz E. Translational readthrough potential of natural termination codons in eucaryotes–The impact of RNA sequence. RNA Biol 2015;12(9):950–8.
[50] Keeling KM, et al. Suppression of premature termination codons as a therapeutic approach. Crit Rev Biochem Mol Biol 2012;47(5):444–63.
[51] Dabrowski M, Bukowy-Bieryllo Z, Zietkiewicz E. Advances in therapeutic use of a drug-stimulated translational readthrough of premature termination codons. Mol Med 2018;24(1):25.
[52] Tork S, et al. The major 5′ determinant in stop codon read-through involves two adjacent adenines. Nucleic Acids Res 2004;32(2):415–21.
[53] Xue X, et al. Identification of the amino acids inserted during suppression of CFTR nonsense mutations and determination of their functional consequences. Hum Mol Genet 2017;26(16):3116–29.
[54] Floquet C, et al. Statistical analysis of readthrough levels for nonsense mutations in mammalian cells reveals a major determinant of response to gentamicin. PLoS Genet 2012;8(3):e1002608.
[55] Clancy JP, et al. Evidence that systemic gentamicin suppresses premature stop mutations in patients with cystic fibrosis. Am J Respir Crit Care Med 2001;163(7):1683–92.
[56] Qian Y, Guan MX. Interaction of aminoglycosides with human mitochondrial 12S rRNA carrying the deafness-associated mutation. Antimicrob Agents Chemother 2009;53(11):4612–8.
[57] Crawford DK, et al. Targeting G542X CFTR nonsense alleles with ELX-02 restores CFTR function in human-derived intestinal organoids. J Cyst Fibros 2021;20(3):436–42.
[58] Corrao F, et al. Nonsense codons suppression. An acute toxicity study of three optimized TRIDs in murine model, safety and tolerability evaluation. Biomed Pharmacother 2022;156:113886.
[59] Gonzalez-Hilarion S, et al. Rescue of nonsense mutations by amlexanox in human cells. Orphanet J Rare Dis 2012;7:58.
[60] Mutyam V, et al. Discovery of Clinically Approved Agents That Promote Suppression of Cystic Fibrosis Transmembrane Conductance Regulator Nonsense Mutations. Am J Respir Crit Care Med 2016;194(9):1092–103.
[61] Friesen WJ, et al. The nucleoside analog clitocine is a potent and efficacious readthrough agent. RNA 2017;23(4):567–77.
[62] Coppens M, et al. Etranacogene dezaparvovec gene therapy for haemophilia B (HOPE-B): 24-month post-hoc efficacy and safety data from a single-arm, multicentre, phase 3 trial. Lancet Haematol 2024;11(4):e265–75.
[63] Frangoul H, et al. Exagamglogene Autotemcel for Severe Sickle Cell Disease. N Engl J Med 2024;390(18):1649–62.
[64] Sun Y, et al. In vivo editing of lung stem cells for durable gene correction in mice. Science 2024;384(6701):1196–202.